Kinetics of the Anodic Dimerization of 4,4′-Dimethoxystilbene by the Rotating Ring-Disk Electrode

Gerd Burgbacher and Hans J. Schäfer*

Contribution from the Organisch-Chemischen Institut, Universität Münster, D-4400 Münster, West Germany. *Received April 30, 1979*

Abstract: The mechanism of anodic coupling of 4,4′-dimethoxystilbene (DMOS) has been studied with the rotating ring-disk electrode (RRDE). DMOS is oxidized at +0.92 V vs. SCE in a one-electron transfer to its radical cation ($DMOS^{+\cdot}$). Simulation of the RRDE results shows that $DMOS^{+\cdot}$ dimerizes in 0.1 M lithium perchlorate–acetonitrile mainly by a radical pathway with $k_2 = 1.59 \times 10^4\ M^{-1}\ s^{-1}$. As the minor parallel reaction, an ECE mechanism has to be assumed with electrophilic attack of $DMOS^{+\cdot}$ at either DMOS ($k_1 = 5 \times 10^3\ M^{-1}\ s^{-1}$) or water ($c_{H_2O}k_3 = 7\ s^{-1}$).

Introduction

Olefins (**1**) with electron-donating substituents (Y = OR,[1] phenyl,[2] vinyl[3]) are dimerized anodically to synthetically useful compounds (eq 1), e.g., 1,4-dicarbonyl compounds **3a**, substituted 1,4-diphenylbutanes **3b**, or octadienes **3c**.

Results of preparative scale electrolysis[2,3] indicate that anodic dimerization of olefins like that of styrene or 1,3-butadiene takes place by electrophilic attack of the primary intermediate, the olefin cation radical (eq 1, path A) and by

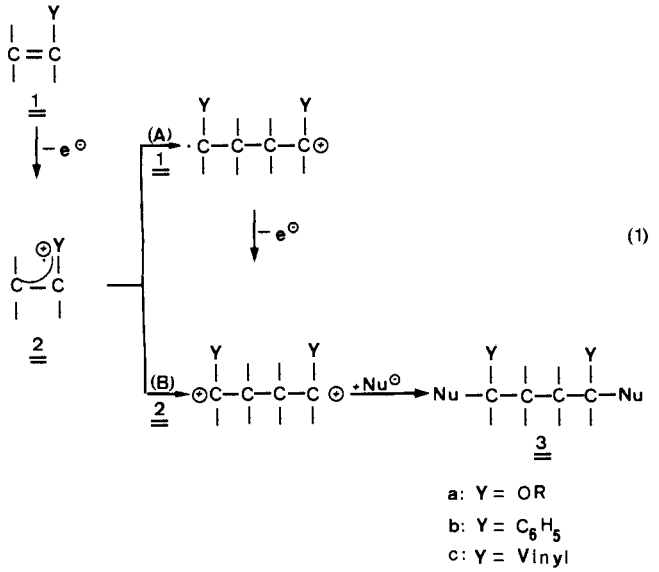

(1)

radical dimerization (path B). This proposition has to be supported by kinetic experiments. The rotating ring-disk electrode (RRDE) allows one to distinguish between the different dimerization mechanisms.[4] Because of the high reactivity of preparatively useful radical cations, the selection of suitable olefins for RRDE experiments is very limited. The severest restriction for quantitative analysis is the formation of polymers that cover the electrode surface and thus falsify the current. Such filming we encountered with *p*-methoxystyrene,[5] ethyl vinyl ether, methyl 3-benzylaminocrotonate, and *p*-methoxy-α-methylstyrene.

4,4′-Dimethoxystilbene (DMOS) has been found suitable for quantitative analysis at the RRDE. It does not cover detectably the electrode; its radical cation has a sufficient lifetime and dimerizes even in the presence of a nucleophile.[6]

Experimental Section

The electrochemical cell for all RRDE experiments consists of a 250-mL flask with one central joint (NS 29) for the rotating electrode and smaller ones for the counter and reference electrodes and the nitrogen inlet. To make the rotating assembly air tight, a Teflon stopper was fitted into the central joint. The stopper had a boring the diameter of which was 0.5 mm larger than that of the electrode shaft. A nitrogen stream was pressured into the slit between the electrode shaft and the Teflon stopper in order to prevent moisture from penetrating into the cell.

The platinum–Teflon rotating ring-disk electrode (Pine Instrument Co., Grove City, Pa., Model DT6) had a disc radius of 0.383 cm, an inner ring radius of 0.399 cm, and an outer ring radius of 0.422 cm. The N value for this electrode, determined from the geometry,[7] was found to be 0.178; experimental measurements with the model systems ferrocene in 0.1 M $LiClO_4$–CH_3OH and 9,10-diphenylanthracene (first wave) in 0.1 M $TBABF_4$–CH_3CN yielded an N value of 0.180 ± 0.005.

The electrode was rotated by using an ASR rotator constructed by the Pine Instrument Co.

The determination of the ring and disk currents was made by two separate circuits. The disk circuit was controlled by a PAR 173 potentiostat/galvanostat (Princeton Applied Research Corp., Princeton, N.J.), whereas the ring circuit was controlled by a Wenking potentiostat LB75L (Fa. Bank, Göttingen). A Wavetek Model 133 function generator provided a dc ramp to drive either the PAR 173 or the LB75L. A Hewlett Packard Model 7046A dual pen xyy recorder was used to record the disk and ring currents simultaneously.

Two Ag/0.1 N $AgNO_3$ electrodes served as reference electrodes. Connection to the solution was made by two Luggin capillaries. The auxiliary electrodes consisted of two platinum nets. During the experiments, the surface of the solution was continuously flushed with purified nitrogen.

In order to obtain N_k values, the disk current was varied stepwise between zero and the limiting current of the first anodic wave. The ring electrode was maintained at a controlled potential so that no ring current was obtained with the disk current being zero.[8] All potentials are referred to the saturated calomel electrode (SCE).

The water content of the solvent acetonitrile was determined by gas chromatography (Model F7, Perkin-Elmer): 2 m × 2 mm Poropak Q column; column temperature, 120 °C; detector temperature, 260 °C; H_2 flow, 130 mL min^{-1}.

Acetonitrile (Merck) was purified according to Mann et al.[9] It was dried over activated alumina before use. $LiClO_4$ (Riedel de Haën) was used without further purification. The salt was dried under vacuum at 150 °C for 2 days. 4,4′-Dimethoxystilbene (Aldrich) was recrystallized twice from benzene.

Results and Discussion

The cyclic voltammogram of DMOS at Pt in 0.1 M $LiClO_4$–CH_3CN (Figure 1) shows two anodic waves with peak potentials of +0.92 and +1.15 V vs. SCE. One electron is transferred at the first wave as shown by comparing the peak height with that for the oxidation of 9,10-diphenylanthracene under identical conditions which exhibits a reversible one electron oxidation in CH_3CN. The second wave is caused by

0002-7863/79/1501-7590$01.00/0

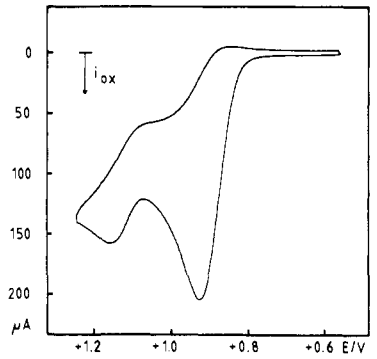

Figure 1. Cyclic voltammogram of 1.0 mM DMOS in 0.1 M $LiClO_4$-CH_3CN solution; voltage scan was at 25 mV s^{-1}.

Table I. Typical Rotating Ring Disk Results for the First Oxidation Wave[a] of 4,4'-Dimethoxystilbene (DMOS)

DMOS concn, mM	$i_{d,l}$, μA	ω, s^{-1}	$i_{d,l}/(c\sqrt{\omega})$, μA mM^{-1} $s^{1/2}$	i_r, μA	N_k
1.02	425	104.72	40.72	31	0.073
	600	209.44	40.65	55	0.092
	730	314.19	40.39	75	0.103
	850	418.88	40.72	95	0.112
	950	523.60	40.70	118	0.124
	1028	628.32	40.21	133	0.129
	1124	733.04	40.70	146	0.130
	1191	837.76	40.34	157	0.132
	1250	924.48	40.31	168	0.134
	1330	1047.20	40.29	180	0.135

[a] The solution was 0.1 M $LiClO_4$ in CH_3CN. The RRDE radii were: r_1 = 0.383 cm; r_2 = 0.399 cm; r_3 = 0.422 cm.

the oxidation of the cation radical to the dication. The smaller peak height indicates that the radical cation undergoes a chemical reaction during the period of voltage scan.[6] At scan rates greater than 320 mV s^{-1}, a new peak appears at 0.86 V because of the reduction of the radical cation. The formation of the tetrahydrofuran derivative **4** has been reported[10] to be the main product (eq 2) of the anodic oxidation of DMOS in

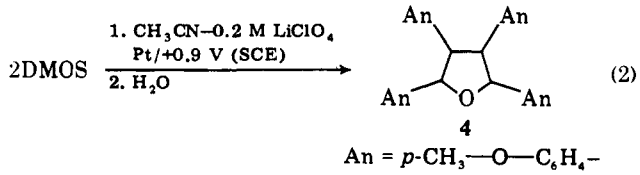

(2)

0.2 M $LiClO_4$-CH_3CN at the potential of the first anodic wave. One Faraday per mole of substrate has been consumed during exhaustive electrolysis. The formation of the product **4** can occur via path A or B (eq 1).

RDE experiments show that the limiting current for the first wave conforms closely to the Levich equation for different values of ω (Table I). The variation of the concentration is limited by the small solubility of DMOS in CH_3CN.

The RRDE experiment is expected to give insight in the dimerization mechanism of the DMOS cation radical. Figure 2 illustrates a typical RRDE voltammogram of DMOS. The disk potential is scanned from 0.6 to 1.4 V, while the ring is maintained at a constant potential of 0.6 V. The ring current increases with increasing disk potential because of the reduction of the radical cation. At sufficient positive potentials, the dication is formed and the ring current drops off.

At the start of this investigation, the reproducibility of the ring current was not sufficient. The i_r-E_d curve shifted to lower i_r values with increasing time, whereas the i_d-E_d curve remained constant. It could be shown that small amounts of

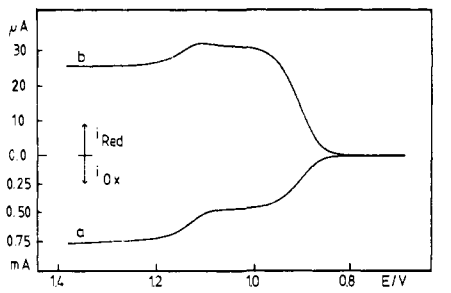

Figure 2. DMOS (1 mM) RRDE voltammogram in 0.1 M $LiClO_4$-CH_3CN solution; ω = 104.72 s^{-1}; (a) i_d vs. E_d and (b) i_r vs. E_d; E_r = 0.6 V.

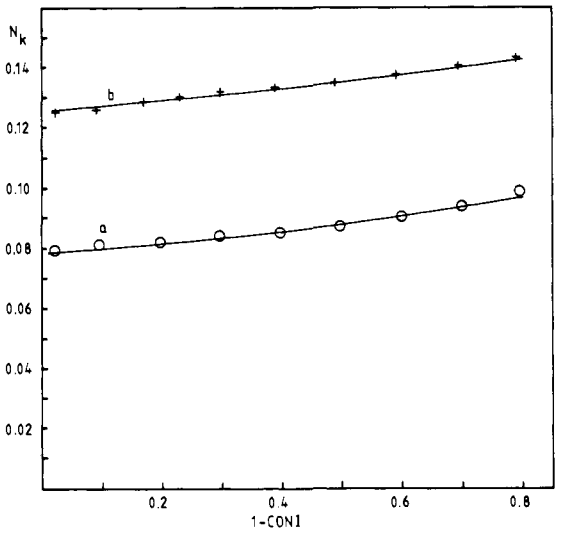

Figure 3. Collection efficiency N_k vs. 1-CONI for a 1.0 mM DMOS solution in 0.1 M $LiClO_4$-CH_3CN at ω = 523.6 s^{-1} (+) and ω = 104.7 (○). Solid lines are theoretical curves corresponding to radical dimerization 4 with participation of reaction 2; $k_1 = 0.3k_2$. (a) XKTC = 1.15 and (b) XKTC = 0.30.

water shifted the i_r-E_d curve in the same direction. This indicates that condensation water probably caused this effect. It was minimized by carefully sealing the cell.

The collection efficiency N_k, defined by $N_k = |i_r/i_d|$, increases with increasing rotation rate (Table I). This behavior is usually observed if a chemical follow up reaction is consuming the product of the electrochemical reaction at the disk electrode forming a species which is not electroactive at the ring. Determination of the collection efficiency for various values of i_d below the limiting current $i_{d,l}$($i_d < i_{d,l}$) allows one to discriminate between different mechanisms of dimerization. Plots of the collection efficiency N_k vs. the disk current function 1-CONI = $1 - (i_d/i_{d,l})$ (CONI expresses the fraction of the limiting current that flows at this voltage) are to be compared with digitally simulated dimensionless working curves of N_k vs. 1-CONI.

The simulation[11] requires the use of dimensionless parameters. For the normalized radii of the electrode, IR1 = 200, IR2 = 208, and IR3 = 220, a collection efficiency, N_0 = 0.177, was simulated that agrees well with the experimental value N_0 = 0.180 ± 0.005. All dimensionless diffusion coefficients were chosen as 0.45. The rate constant is included in a dimensionless variable which is defined as $XKTC = 0.51^{-2/3}\nu^{1/3}D^{-1/3}\omega^{-1}kc^b$, where ν is the kinematic viscosity (ν = 0.0045 centistokes), D the diffusion coefficient of the parent molecule ($D = 1.61 \times 10^{-5}$ cm^2 s^{-1} determined from $i_{d,l}$ and the Levich equation), ω the radical velocity (s^{-1}), k the second-order rate constant (M^{-1} s^{-1}), and c^b the bulk concentration (M).

Typical experimental results are shown in Figure 3 (ω =

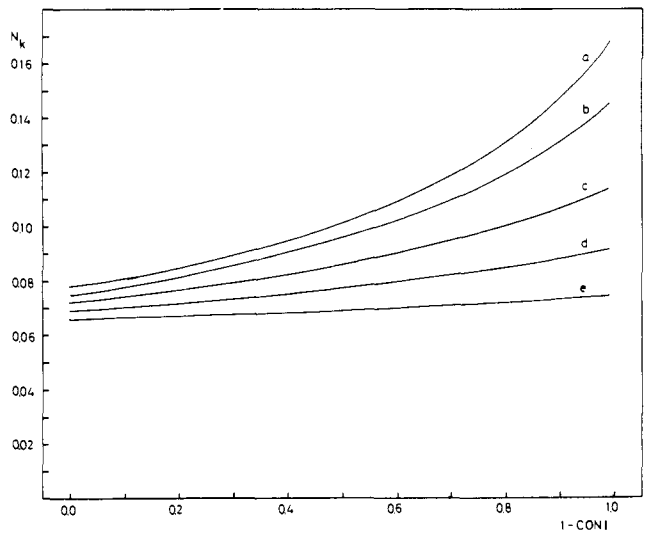

Figure 4. Simulated plots of collection efficiency vs. 1-CONI for a radical dimerization according to reaction 4 with increasing participation of reaction 2. XKTC = $0.51^{-2/3}\nu^{1/3}D^{-1/3}\omega^{-1}c^{b}k_2$. XKTC1 = $0.51^{-2/3}\nu^{1/3}D^{-1/3}\omega^{-1}c^{b}k_1$. XKTC = 1.5; XKTC1 = (a) 0.0; (b) 0.1; (c) 0.3; (d) 0.5; (e) 0.7.

Table II. Calculated Rate Constants of 4,4'-Dimethoxystilbene Radical Cation Obtained from RRDE Results in 0.1 M $LiClO_4$–CH_3CN Solutions[a]

ω,[a] s^{-1}	c, mM	XKTC[b]	k_2,[c] $M^{-1}\,s^{-1}$
104.72	0.85	1.15	1.38×10^4
	1.00	1.60	1.64
	1.07	1.30	1.24
	1.00	1.40	1.43
	1.00	1.50	1.53
	1.00	1.60	1.64
523.60	0.85	0.30	1.80
	1.00	0.38	1.94
	1.07	0.33	1.69
	1.00	0.32	1.64
		av: 1.59×10^4	
		SD: 0.19×10^4	

[a] The RRDE had: $r_1 = 0.383$ cm; $r_2 = 0.399$ cm; $r_3 = 0.422$ cm. [b] XKTC = $0.51^{-2/3}\nu^{1/3}D^{-1/3}\omega^{-1}c^{b}k_2$; $\nu = 0.0045$ cm^2 s^{-1}; $D = 1.61 \times 10^{-5}$ cm^2 s^{-1}. [c] Rate constant for radical dimerization.

104.72 (○); ω = 523.60 (+)). N_k decreases with increasing CONI. This trend is characteristic for a radical dimerization and excludes an ECE mechanism according to Scheme I. Simulated working curves for a pure radical dimerization (Scheme II) are too steep compared with experimental data. A better fit is obtained by assuming that reaction 2 takes place parallel to radical dimerization. Figure 4 shows the change in the working curves with increasing participation of reaction 2 (only $DMOS^{+\cdot}$ is assumed to be reduced at the ring). The simulated rate law for the disappearance of the radical cation is:

$$d[DMOS^{+\cdot}]/dt = -2k_2[DMOS^{+\cdot}]^2 - k_1[DMOS][DMOS^{+\cdot}] \quad (6)$$

A good fit of the working curves with experimental points is achieved if $k_1 = 0.3k_2$ (Figure 3).

Table II shows values for XKTC and k_2 for different values of the rotation speed. The variation of the concentration is limited by the small solubility of DMOS in CH_3CN. The average value of k_2 obtained from these data is 1.59×10^4 M^{-1} s^{-1}. Mechanism and kinetic data are in good agreement with

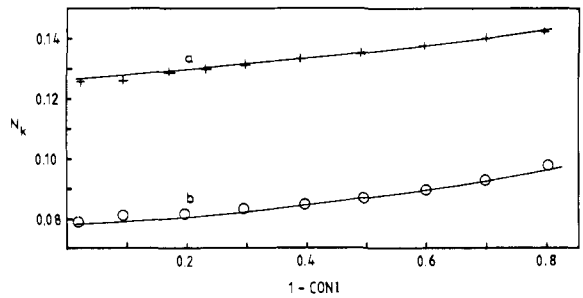

Figure 5. Digitally simulated working curves for a radical dimerization paralleled by electrophilic attack of the radical cation on water and observed experimental values (0.85 mM DMOS in CH_3CN–0.1 M $LiClO_4$); $\omega = 523.65$ s^{-1} (+) and $\omega = 104.7$ s^{-1} (○). XKTC = (a) 0.18; (b) 0.60. XKTC3 = (a) 0.01; (b) 0.04. CXFRAC = (a) 15.0; (b) 15.0. XKTC3 = $0.51^{-2/3}\nu^{1/3}D^{-1/3}\omega^{-1}c_{H_2O}k_3$. CXFRAC = c_{H_2O}/c_{DMOS}. IR1 = 200. IR2 = 208. IR3 = 220.

Scheme I. ECE Dimerization

$$DMOS \rightleftharpoons DMOS^{+\cdot} + e^- \quad (1)$$

$$DMOS^{+\cdot} + DMOS \xrightarrow{k_1} (DMOS)_2^{+\cdot} \quad (2)$$

$$(DMOS)_2^{+\cdot} \rightleftharpoons (DMOS)_2^{2+} + e^- \quad (3)$$

Scheme II. Radical Dimerization

$$DMOS \rightleftharpoons DMOS^{+\cdot} + e^- \quad (1)$$

$$2\ DMOS^{+\cdot} \xrightarrow{k_2} (DMOS)_2^{2+} \quad (4)$$

$$(DMOS)_2^{2+} \longrightarrow Prod \quad (5)$$

Scheme III. Hydrolysis

$$DMOS \rightleftharpoons DMOS^{+\cdot} + e^- \quad (1)$$

$$DMOS^{+\cdot} + H_2O \xrightarrow{k_3} DMOS(OH)^{\cdot} + H^+ \quad (7)$$

$$2\ DMOS(OH)^{\cdot} \longrightarrow Prod \quad (8)$$

Table III. Calculated Values for XKTC,[a] XKTC3, and CXFRAC, k_2 and k_3 According to Rate Law 9

ω, s^{-1}	c_{DMOS}, mM	XKTC	XKTC3	CXFRAC	$k_2 \times 10^{-3}$, $M^{-1}\,s^{-1}$	$k_3 \times 10^{-3}$, $M^{-1}\,s^{-1}$	c_{H_2O}, mM	$c_{H_2O} \times k_3$, s^{-1}
104.72	0.85	0.6	0.1	6.0	7.2	1.20	5.1	6.12
		0.6	0.04	15.0		0.48	12.75	6.12
		0.6	0.02	30.0		0.24	25.5	6.12
523.60		0.18	0.028	6.0	11.0	1.70	5.1	8.67
		0.18	0.011	15.0		0.66	12.75	8.42
		0.18	0.0055	30.0		0.33	25.5	8.42

[a] XKTC: standardized form of the rate constant k_2. XKTC3: standardized form of the rate constant k_3. CXFRAC: standardized water concentration (CXFRAC = C_{H_2O}/C_{DMOS}).

the spectroelectrochemical study of the anodic dimerization of DMOS.[10]

There might be another explanation for the flattened curves compared with those of a pure radical dimerization: the dimerization of DMOS cation radical is paralleled by the irreversible reaction of $DMOS^{+}\cdot$ with water (Scheme III). This assumption is strongly supported by the observed influence of water on the ring current as indicated above. Although every effort had been made to minimize the penetration of water into the cell during the measurements, there might be a considerable amount of residual water in the solvent CH_3CN. Gas chromatographic analysis of solutions after an RRDE experiment indicated water contents between 15 and 25 mM. Even carefully dried CH_3CN contains about 5 mM of water. A consequence of this is that, even under optimal conditions, the water concentration exceeds that of DMOS.

If the first-order disappearance of the cation radical via the ECE sequence (Scheme I) is replaced by first-order electrophilic attack of the cation radical on water (Scheme III), rate law 9 is obtained:

$$d[DMOS]/dt = -k_2[DMOS^{+}\cdot]^2 - k_3[DMOS^{+}\cdot][H_2O] \quad (9)$$

The simulation of the radical dimerization paralleled by the reaction of the cation radical with water was carried out under the assumption that the product of the reaction of $DMOS^{+}\cdot$ with water is electroinactive at the disk and at the ring. Curves, generated for this mechanism, which fit closely to the experimental points, are represented in Figure 5.

The fit could be achieved with different amounts of water (CXFRAC = $[H_2O]/[DMOS]$) if the product $[H_2O]k_3$ is constant. This is shown in Table III. The value of k_2 is held constant for a given ω. A small drift in the rate constant k_2 and the product $[H_2O]k_3$ has been observed for different values of ω. This drift could be eliminated by better adjustment of the rate constant k_2. The average value for k_2 is $9 \times 10^3\ M^{-1}\ s^{-1}$ and that for $k_3[H_2O]$ is $7\ s^{-1}$.

Conclusion

4,4'-Dimethoxystilbene (DMOS) is being oxidized at + 0.92 V vs. SCE to its radical cation ($DMOS^{+}\cdot$). RRDE experiments prove that $DMOS^{+}\cdot$ couples mainly by a radical dimerization with an average rate constant of $k_2 = 1.59 \times 10^4\ M^{-1}\ s^{-1}$. As the minor parallel reaction, an ECE mechanism with electrophilic attack of $DMOS^{+}\cdot$ at either DMOS ($k_1 = 5 \times 10^3\ M^{-1}\ s^{-1}$) or water ($c_{H_2O}k_3 = 7\ s^{-1}$) has to be assumed. The water content of the electrolyte determined by GLC analysis could not be reduced below 15 mM. A clear distinction between these two alternative parallel reactions is not possible, because for each water concentration a rate constant for the reaction of $DMOS^{+}\cdot$ with water can be evaluated which can be fitted to the experimental values.

The mechanism for the DMOS dimerization certainly cannot be generalized. The product structures in the preparative scale coupling of enamino ketones or esters also make a radical dimerization[12] probable, while the results with styrene derivatives,[2] 1,3-dienes,[3] and enol ethers[1] indicate an ECE mechanism. However, the latter olefins could not be investigated with the rotating ring disk electrode. In acetonitrile, an electrolyte of low nucleophilicity, the electrode is severely filmed, while in methanol where only little filming occurs the rates are too high for RRDE detection.

Acknowledgment. We thank the Deutsche Forschungsgemeinschaft and the Fonds der chemischen Industrie for generous support of this work and Dr. E. Steckhan for helpful discussions.

References and Notes

(1) D. Koch, H. Schäfer, and E. Steckhan, *Chem. Ber.*, **107**, 3640 (1974).
(2) R. Engels, H. Schäfer, and E. Steckhan, *Justus Liebigs Ann. Chem.*, 204 (1977).
(3) H. Baltes, E. Steckhan, and H. J. Schäfer, *Chem. Ber.*, **111**, 1294 (1978).
(4) V. J. Puglisi and A. J. Bard, *J. Electrochem. Soc.*, **119**, 833 (1972).
(5) L. Eberson and V. D. Parker, *Acta Chem. Scand.*, **24**, 3553 (1970).
(6) V. D. Parker and L. Eberson, *J. Chem. Soc., Chem. Commun.*, 340 (1969).
(7) W. J. Albery and M. L. Hitchman, "Ring-Disc Electrodes", Oxford University Press, Oxford, 1971, p 8.
(8) V. J. Puglisi and A. J. Bard, *J. Electrochem. Soc.*, **119**, 829 (1972).
(9) J. F. O'Donnel, J. T. Ayres, and C. K. Mann, *Anal. Chem.*, **37**, 1161 (1965).
(10) E. Steckhan, *J. Am. Chem. Soc.*, **100**, 3526 (1978).
(11) K. B. Prater and A. J. Bard, *J. Electrochem. Soc.*, **117**, 207 (1970).
(12) D. Koch and H. Schäfer, *Angew. Chem., Int. Ed. Engl.* **12**, 245 (1973).